

EXTRACTION OF HORIZONTAL VANISHING LINE USING SHAPES AND STATISTICAL ERROR PROPAGATION

L. Havasi *, T. Szirányi

Hungarian Academy of Science, H-1111 Kende utca 13-17 Budapest, Hungary - (havasi, sziranyi)@sztaki.hu

Commission III

KEY WORDS: geometrical scene analysis, error propagation, video processing, Hough transformation

ABSTRACT:

In this paper we address the problem of estimating the horizontal vanishing line, making use of motion statistics derived from a video sequence. The computation requires the satisfying of a number of corresponding object's height measurement; and in our approach these are extracted using motion statistics. These easy-to-compute statistics enable accurate determination of average shape of every point in the image. Thanks to the use of motion statistics and error propagation formulas in the intermediate steps, our approach gives robust results. The outcomes show that our approach gives accurate results in the context of different environments.

1. INTRODUCTION

In recent years there has been a dramatic increase in the number of video surveillance systems in use; and these have in turn generated a large quantity of archived video recordings, which are usually stored without any image-processing. In most cases for such recordings one does not know the relative and global geometrical properties of the surveillance cameras.

Despite this, there is a striking lack of publications concerning the extraction of geometric characteristics from images contained in video recordings. We may note that this task is much simplified in the case where some known test object is used during system calibration. In this paper however a statistical framework is introduced which allows us, without such calibration to derive the horizontal vanishing line (VL). The vanishing line is useful for camera orientation and extrinsic parameter determination (Lu et al., 2002). For still images (Criminisi et al., 1999), it can be successfully determined only when there are detectable parallel lines; and in image-sequences, only when certain assumptions are satisfied which enable us to detect and track known objects (Lu et al., 2002). In summary, most of the published still-image based methods are unsuitable for processing the images of a typical surveillance scene. Furthermore, in typical surveillance scenes of public places the assumptions on which the video-based methods are posited are not satisfied.

The main practical advantage of our proposed method is that there is no need for any time-consuming processing steps. Furthermore because of the statistical method employed it is a robust procedure, and sub-pixel accuracy may be achieved. These properties are especially important in the analysis of outdoor surveillance videos. In videos captured by analog surveillance cameras the contrast and focus are often badly adjusted, and thus precise measurements are not possible in individual frames. This consideration led to our concept of summarizing the information from a sequence of a number of frames (as many as possible) in order to achieve higher accuracy in the averaged retrieved information. The paper introduces a parameter-optimization approach which is

appropriate to this statistical feature-extraction method; and thus we establish a framework for estimation of the parameters in a slightly different way to other parameter optimization methods (Nguyen et al., 2005; Ji and Xie, 2003).

The parameter estimation method we introduce here applies simple outlier rejection step prior to the nonlinear optimisation. Another advantage of the method is that it is capable of working on low frame-rate videos, since the relevant parameter for the statistical information extraction is not the refresh rate itself, but rather the total frame-count of the processed sequence.

2. PROBLEM DESCRIPTION

Parallel planes in a 3-dimensional space intersect a plane at infinity in a common line, and the image of this line is the horizontal vanishing line, or horizon. The vanishing line (VL) depends only on the orientation of the camera (Hartley and Zisserman, 2000). In the paper we describe the VL with the parameters of the line.

In summary, the determination of the vanishing line is possible with knowledge of at least two vanishing points (these lie in the VL); thus three corresponding line segments (e.g. derived from the height of a given person in the image), or else known parallel lines in the same plane, are necessary.

These line segments can be computed from the apparent height of the same object as seen at different positions (depths) on the ground-plane. The objects may for instance be pedestrians (Lu et al., 2002), and the line segments denote their height. However, the precise detection of such non-rigid objects is a challenging task in outdoor images.

3. PROPOSED METHOD

In this section we introduce a novel solution based on our previous results on motion statistics to derive shape information from videos. The statistical properties of uncertainty of extracted information have been successfully used for accurate parameter estimation.

* Corresponding author.

3.1 Extraction of Shape Properties

Our feature-detection method is based on the use of so-called co-motion statistics (Szlávik et al., 2004). These statistics have been successfully used for image registration in the case of wide-baseline camera pairs and for vanishing point determination in camera-mirror settings (Havasi and Szirányi, 2006). Briefly, these statistics are a numerical estimation of the concurrent motion probability of different pixels in the camera plane

A straightforward step is that the input is some motion mask which is extracted using a suitable algorithm, which may be any one of the several methods available (Cucchiara et al., 2003).

The temporal collection of 2D masks provides useful information about the parts of the image where spatially-concurrent motion occurs, and thereby about the scene geometry. These statistics come from the temporal summation of the binarized masks; these mask are written $m(t, \mathbf{x})$ where t is the time and the 2D vector \mathbf{x} is the position in the image. Thus, these masks comprise a set of elements signifying motion (“1”) or no-motion (“0”). The co-motion statistics in *local* sense can be summarized with the following two equations. First, we define the global motion statistics which determines the motion probability in every pixel (because of the discrete time-steps, Δt denotes the frame count):

$$P_g(\mathbf{x}) = \frac{\sum_t m(t, \mathbf{x})}{\Delta t} \quad (1)$$

In general, the concurrent-motion probability of an arbitrary image-point \mathbf{u} with another image-point \mathbf{x} may be defined with the following conditional-probability formula:

$$P_{co}(\mathbf{u}|\mathbf{x}) = \frac{\sum_t m(t, \mathbf{u})m(t, \mathbf{x})}{\sum_t m(t, \mathbf{x})} \quad (2)$$

For a detailed description of the implementation issues, we refer to (Szlávik et al., 2004). After normalization

$$\sum_{\mathbf{u}} P_{co}(\mathbf{u}|\mathbf{x}) = 1 \quad (3)$$

the $P_{co}(\cdot)$ is assigned to every pixel in the image, the 2D discrete PDF (probability distribution function) will provide useful information about the shapes: the average shape can be determined, because $P_{co}(\mathbf{u}|\mathbf{x})$ collects information about objects which pass through the point \mathbf{x} . These PDFs may be approximated by normal distributions because the *central limit theorem* says that the cumulative distribution function of independent random variables (each have an arbitrary probability distribution with mean and finite variance) approaches a normal distribution (Kallenberg, 1997). Thus,

$$P_{co}(\mathbf{u}|\mathbf{x}) = N(\mathbf{u}, \boldsymbol{\mu}_x, \boldsymbol{\Sigma}_x) \quad (4)$$

where the normal distribution is defined as

$$N(\mathbf{x}, \boldsymbol{\mu}, \boldsymbol{\Sigma}) = \frac{1}{\sqrt{(2\pi)^2 |\boldsymbol{\Sigma}|}} \exp\left(-\frac{1}{2}(\mathbf{x} - \boldsymbol{\mu})\boldsymbol{\Sigma}^{-1}(\mathbf{x} - \boldsymbol{\mu})\right) \quad (5)$$

The following figure illustrates the results of motion statistics in both indoor and outdoor sequences.



Figure 1. Sample frames in upper row, and raw motion statistics (defined by (2)) in the bottom row. The corresponding point is marked by ‘x’

From this feature extraction the input for the further processing steps is the parameters of the covariance matrix $\boldsymbol{\Sigma}_x$ in point \mathbf{x} . The dimensions and orientation of the average shape come from the eigen-value decomposition of the covariance matrix:

$$\boldsymbol{\Sigma}_x \mathbf{v}_{x,i} = \lambda_{x,i} \mathbf{v}_{x,i} \quad i = 1, 2 \quad (6)$$

These statistical characteristics are displayed in figure 2.

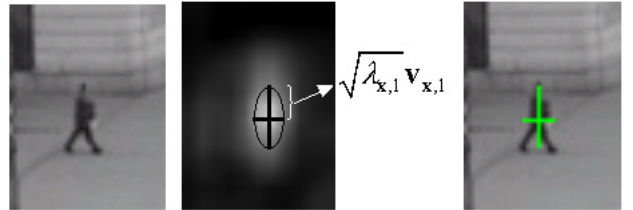


Figure 2: Example to shape properties: axes of normal distributions, derived from the eigen-value decomposition of the covariance matrix.

Finally, the height measurement comes from the projection (vertical component) of the most vertical eigenvector:

$$(\lambda_{x,\max}, \mathbf{v}_{x,\max}) = \arg \max_{(\lambda, \mathbf{v})} (\lambda_{x,1} \langle \mathbf{e}, \mathbf{v}_{x,1} \rangle, \lambda_{x,2} \langle \mathbf{e}, \mathbf{v}_{x,2} \rangle) \quad (7)$$

$$h_j = h_x = \sqrt{\lambda_{x,\max}} \langle \mathbf{e}, \mathbf{v}_{x,\max} \rangle$$

where \mathbf{e} denotes the vertical unit vector: $\mathbf{e} = [0 \ 1]$ and $\langle \cdot \rangle$ is the dot product, respectively. These height estimations are displayed in figure 3. For the sake of later simplification we transform the indices from vector (coordinate) form e.g. \mathbf{x} to a simple scalar index j . Henceforward, j denotes a point in the

image; viz. h_j is the height measurement in image-point j and vector \mathbf{p}_j determines the coordinates of point j in the image. Because the scheme (7) utilizes information extracted from statistics, a more sophisticated form may be given for the height estimation which takes into account the uncertainty:

$$P(\hat{h}_j | h_j) = N(\hat{h}_j, h_j, \Sigma_{\Delta h_j}) \quad (8)$$

where

$$\Sigma_{\Delta h_j} = \sigma_{\Delta h_j}^2 = (\sqrt{\lambda_{j,\max}} - h_j)^2 \quad (9)$$

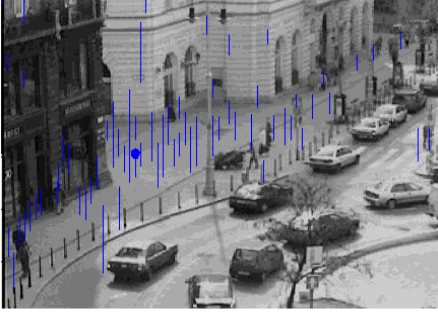


Figure 3: Odd sample from height estimations in outdoor environment.

3.2 Outlier Rejection

In summary, the determination of the vanishing line is possible with knowledge of at least three corresponding line segments. In our framework the necessary height information can be easily determined from the *local* statistics. The information derived from statistics is valid only if the following assumption is satisfied: there are regions where the same objects are moving with equivalent probability (e.g. pathway or road).

In general, without making any prior assumptions about the scene every point may be paired to every other point. But the practical processing of this huge data-set requires that we have an effective way to drop ‘outlier’ points and extract information for VL estimation.

First, we describe simple conditions which can be used to reduce the size of the data-set. The outlier rejection in this case is similar to dropping points where two objects are moving but are not the same size. Let j represents an arbitrary point in the image and k denotes another (corresponding) point: $j \neq k$

We reckon two points as corresponding points (which is probable, where same-sized objects are concerned) if

$$\sigma_1 < \frac{\lambda_{j,1}}{\lambda_{j,2}} / \frac{\lambda_{k,1}}{\lambda_{k,2}} < \sigma_2 \quad (10)$$

and

$$\Phi(\mathbf{v}_{j,1}, \mathbf{v}_{k,1}) < \alpha \quad (11)$$

where the notations come from the eigenvalue decomposition of the covariance matrices of two points, see (6), and $\Phi(\cdot)$ denotes the angle between two vectors (the deviation of

eigenvectors in our case). These simple conditions lead to a set of points where the objects have similar orientation and aspect ratio. Figure 4 demonstrates the point set (marked by circles) corresponding to a point (marked by x).



Figure 4: Corresponding points (marked with circles) are related to an arbitrary image point (marked by large ‘x’).

After this preprocessing every point will have several probable corresponding point-pairs. However, several outliers remain, thus we have to use all points to determine vanishing points and an estimation about horizon.

3.3 Error Propagation

An initial guess about the horizon can be computed using the height information of corresponding points to an arbitrary point j :

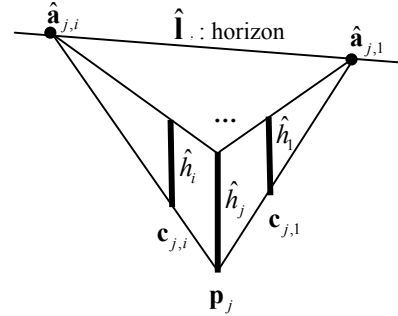


Figure 5. Using vertical size information to get the horizon ($\hat{\mathbf{i}}_j$) and vanishing points $\hat{\mathbf{a}}_{j,i}$. The 2D point \mathbf{p}_j is an arbitrary image point, while $\mathbf{c}_{j,1}$ and $\mathbf{c}_{j,i}$ are two samples for corresponding points determined in the previous section.

To simplify the further computations the transformation between height information and the 2D image plane is necessary. We have to compute point coordinates in the ground-plane, as it is demonstrated in the following figure.

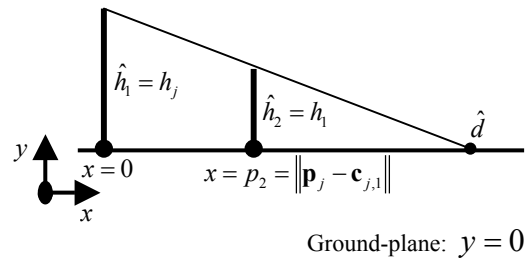


Figure 6. Determination of a vanishing point, which in ideal case lies in the horizontal vanishing line (horizon). The task may be summarized as the computation of \hat{d} taking into account the inaccuracy of height measurements.

The determination of \hat{d} without uncertainty comes from elementary algebra:

$$\hat{d} = \hat{h}_1 \frac{p_2}{\hat{h}_1 - \hat{h}_2} \quad (12)$$

To derive a formula which contains the uncertainty – based on the method described in (Ji and Xie, 2003) – we define the relationship between the input and the output quantity in an implicit form. For this scheme we define the ideal input vector \mathbf{X} and the observed vector $\hat{\mathbf{X}}$. The ideal parameter vector Θ and the observed $\hat{\Theta}$, respectively. The $\hat{\Theta}$ and $\hat{\mathbf{X}}$ are related through an optimisation function $F(\cdot)$, and $\hat{\Theta}$ is determined by minimising $F(\hat{\mathbf{X}}, \hat{\Theta})$. In this phase of our method the input measurements are height information about the objects, while the output is the estimated position of the intersection of ground plane and the line through points $(0, \hat{h}_1)$ and (p_2, \hat{h}_2) , see figure 6. This line-plane intersection determines one point, accordingly the input vector is

$$\hat{\mathbf{X}} = [\hat{h}_1, \hat{h}_2] \quad (13)$$

and the observation is

$$\hat{\Theta} = [\hat{d}] \quad (14)$$

The analytic curve function expressed as

$$F(\hat{\mathbf{X}}, \hat{\Theta}) = \hat{h}_1(p_2 - \hat{d}) - \hat{h}_2(p_1 - \hat{d}) = 0 \quad (15)$$

Error propagation relates the uncertainty of input measurements to the perturbation of $\hat{\Theta}$. Let $\Sigma_{\Delta X}$ be the covariance matrix of measurements:

$$\Sigma_{\Delta X} = \begin{bmatrix} \sigma_{\Delta X}^2 & 0 \\ 0 & \sigma_{\Delta X}^2 \end{bmatrix} \quad (16)$$

where

$$\sigma_{\Delta X}^2 = \frac{\sigma_{\Delta h_j}^2 + \sigma_{\Delta h_k}^2}{2} \quad (17)$$

Based on the covariance propagation theory (Haralick, 1994), we have

$$\Sigma_{\Delta \Theta} = 2\sigma_{\Delta X}^2 \left[\left(\frac{\partial g}{\partial \Theta} \right)^T \right]^{-1} \quad (18)$$

where $\frac{\partial g(\mathbf{X}, \Theta)}{\partial \Theta}$ is defined as

$$\frac{\partial g}{\partial \Theta} = 2 \frac{\left(\frac{\partial F}{\partial \Theta} \right)^2}{\left(\frac{\partial F}{\partial h_1} \right)^2 + \left(\frac{\partial F}{\partial h_2} \right)^2} \quad (19)$$

Thus, we have

$$\Sigma_{\Delta \Theta} = \sigma_{\Delta \Theta}^2 = \sigma_{\Delta X}^2 \frac{(p_2 - \hat{d})^2 + \hat{d}^2}{(\hat{h}_2 - \hat{h}_1)^4} \quad (20)$$

The result is illustrated in the following figure.

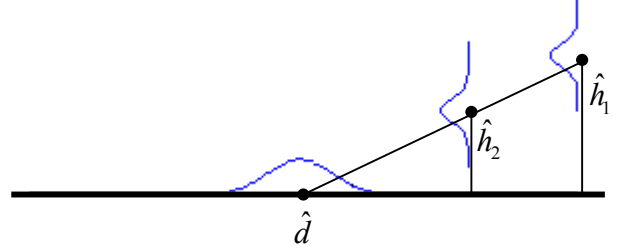


Figure 7. Simulation of error propagation from input data (height estimations) into 1D position coordinate. The two uncertainty heights are used to determine the intersection of line through these points and the x axis. The formula for uncertainty of this intersection was expressed by (20).

Finally, we have to convert the result of (20) into the 2D image plane. This conversion can be accomplished by constructing a 2D covariance matrix:

$$\Sigma_{\Delta VP_{j,i}} = \mathbf{U}^T \begin{bmatrix} \sigma_{\Delta \Theta}^2 & 0 \\ 0 & 0 \end{bmatrix} \mathbf{U} \quad (21)$$

where \mathbf{U} is the matrix of eigen-vectors (Note that, $\mathbf{U}\mathbf{U}^T = \mathbf{I}$):

$$\mathbf{U} = \begin{bmatrix} \mathbf{v}_i \\ \tilde{\mathbf{v}}_i \end{bmatrix} \text{ and } \langle \mathbf{v}_i, \tilde{\mathbf{v}}_i \rangle = 0 \quad (22)$$

with eigen-vectors formed from the unit length vector through points \mathbf{p}_j and $\mathbf{c}_{j,i}$:

$$\mathbf{v}_i = \frac{\mathbf{c}_{j,i} - \mathbf{p}_j}{\|\mathbf{c}_{j,i} - \mathbf{p}_j\|} \quad (23)$$

While the centroid (position of vanishing point defined by points j and i) is determined from the estimated distance \hat{d} along the line with direction \mathbf{v}_i :

$$\hat{\mathbf{a}}_{j,i} = \mathbf{p}_j + \mathbf{v}_i \hat{d} \quad (24)$$

Thus, we have the formula for probability density of measurement noise:

$$P(\hat{\mathbf{a}}_{j,i} | \mathbf{a}_{j,i}) = N(\hat{\mathbf{a}}_{j,i}, \mathbf{a}_{j,i}, \Sigma_{\Delta VP_{j,i}}) \quad (25)$$

3.4 Conversion into Hough-space

After the evaluation of the error propagation formula to every corresponding point pair we will have several uncertain 2D point coordinates. These estimations represent an initial guess about horizon, since the inliers of the data-set lie in the horizon. This line estimation problem is well known and there are several approaches to solve it in various cases: e.g. least squares (LS), total least squares (TLS) and Hough transformation (Kiryati and Bruckstein, 2000; Nguyen et al., 2005).

In short, our case has the following special properties:

1. Error in both coordinates in the 2D plane (x and y).
2. There is correlation between the noise in the two coordinates.
3. The noise covariance matrices are different for different data points (heteroscedastic noise).
4. Notable amount of outliers can be found in the data-set.

Because of these specific characteristics the line fitting is viewed as a global optimisation procedure. Generally, there is no analytic solution for the cases of heteroscedastic and correlated noise, where we assume that the noise in x is correlated to the noise in y, furthermore, the variance of the noise is not identical for all data points. Heteroscedastic regression problem in computer vision is studied in (Kiryati and Bruckstein, 2000). Both LS and TLS methods fail when the data-set contains outliers. Line fitting on such data-set needs a robust estimator, for survey see (Nguyen et al., 2005). The Hough transform is an effective and popular way for line-fitting (Duda and Hart, 1972). In the standard version, an accumulator array is used to collect the points which lie along the same line. The line is parametrized by (θ, ρ) :

$$\rho = x \cos(\theta) + y \sin(\theta) \quad (26)$$

In this section the error propagation will be continued, and an optimal line parameter has been determined by using non-linear optimisation procedure. Because the Hough transformation generates sinusoidal voting patterns in the parameter space we will not use the same error propagation formula as in the previous section. In the end of the section a simple formula for the error estimation in the parameter space will be given.

Let 2D point $\mathbf{a}_{j,i} = (x_i, y_i)$ be the unknown accurate position of the i^{th} vanishing point introduced in the previous section. The measurements are $\hat{\mathbf{a}}_{j,i} = (\hat{x}_i, \hat{y}_i)$ based on the error propagation formula. Due to noise, $\mathbf{a}_{j,i} \neq \hat{\mathbf{a}}_{j,i}$. The probability density of measurement noise is modelled as a 2D heteroscedastic Gaussian, with correlated noise in formula (25). We define the line-fitting task as finding the maximum of the objective function:

$$\hat{\mathbf{l}}_j = \arg \max_{\mathbf{l} \in (\theta, \rho)} \sum_i P_g(\mathbf{p}_i) C_{j,i}(\mathbf{l}) \quad (27)$$

where the maximum value of probability (25) along the line \mathbf{l} is defined by:

$$C_{j,i}(\mathbf{l}) = \max_{\mathbf{u} \in \mathbf{l}} P(\mathbf{u} | \mathbf{a}_{j,i}) \quad (28)$$

(This line is also parametrized by $\hat{\mathbf{l}}_j = (\hat{\theta}_j, \hat{\rho}_j)$.)

The optimum value is determined by *unconstraint non-linear optimisation* of (27), the initial estimate is given by LMS method. The introduced formula handles the outliers, thus there is no need for robust M-estimator, where the error expressions are replaced by some saturation function (Nguyen et al., 2005). We note that, the computation of (28) is simple; it has analytic solution, see (Kiryati and Bruckstein, 2000) for details. Since the residual outliers cause an error in line-fitting, we define the error in line-fitting with a 2D Gaussian:

$$P(\hat{\mathbf{l}}_j | \mathbf{l}_j) = N(\hat{\mathbf{l}}_j, \mathbf{l}_j, \Sigma_{\Delta VL_j}) \quad (29)$$

where the covariance matrix is defined as

$$\Sigma_{\Delta VL_j} = \begin{bmatrix} \tan^{-1}\left(\frac{\Delta l_y}{\Delta l_x}\right)^2 & 0 \\ 0 & \Delta l_x^2 \end{bmatrix} \quad (30)$$

The notations are detailed in the following figure.

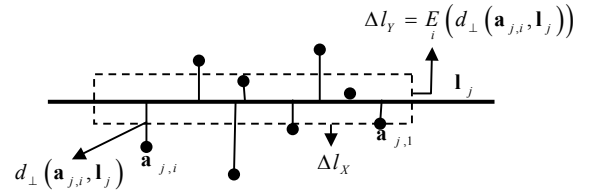


Figure 8. Demonstrating the parameters for the expression of line-fitting error (see (30)) in parameter space.

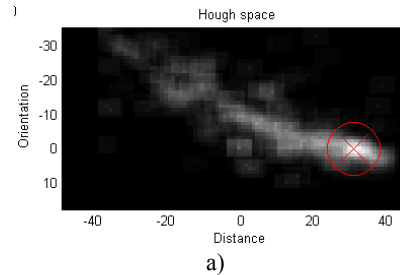
The function $d_{\perp}(\cdot)$ computes the distance between the line \mathbf{l}_j and point $\mathbf{a}_{j,i}$, while the expected value denoted by $E(\cdot)$. Thus, the guess about the horizon at point j is determined by (29) which describes uncertainty in the parameter space (2D Hough-space).

3.5 Final optimization procedure

The estimation about the horizon and the estimation error are attached to several points in the image, as we have introduced it in the previous sections. The accurate determination of horizon is carried out in parameter space using all estimations:

$$\mathbf{l}_h = \arg \max_{\mathbf{l} \in (\theta, \rho)} \sum_i P_g(\mathbf{p}_i) P(\mathbf{l} | \mathbf{l}_i) \quad (31)$$

It has been fulfilled with the same optimisation technique as in previous section. The following figure displays the 2D parameter space which has been filled with numerically computed values of (31).



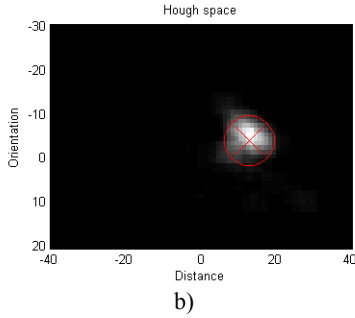


Figure 9: The lower picture in b) depicts the Hough space of indoor, while the upper relates to outdoor scene, respectively.

4. EXPERIMENTAL RESULTS

We performed a practical evaluation of the method in which both indoor and outdoor videos were used as input. The parameters introduced in the previous sections are assigned the following values in empirical fashion: $\sigma_1 = 0.8$ and $\sigma_2 = 1.25$ in (10), while $\alpha = 10^\circ$ in (11). To determine the binary motion mask ($m(t, \mathbf{x})$) a motion-detection method was used which is based on the background model introduced by Stauffer (Stauffer et al., 2000).

The manual extrapolation of the vanishing line is a difficult task, because: i) there are not enough static features for accurate alignment; and ii) the objects are usually too small in case of outdoor images. The outdoor video used for testing shows not only pedestrians, but cars as well; this is why the parameter configurations (distance and orientation of the horizon line) in Hough space show scatter, see figure 9a. The deviation from optimal parameter values is much smaller in indoor case, see figure 9b.

The results demonstrated by straight line in 2D coordinate space after final optimisation of Hough space are displayed in figure 10.



Figure 10: Horizon computation in indoor and outdoor videos.

5. DISCUSSION

An approach for the determination of geometric scene property, namely the horizontal vanishing line (horizon) in image sequences has been introduced. The simple motion statistics are the novel feature used as a basis for estimation of average shape for every point in the image, which provides the necessary height information for the estimation of VPs and finally for the determination of horizon.

We have shown that using the proposed algorithm it is feasible to compute the horizon with good accuracy even from a real-life noisy data set which contains several outliers. The proposed

approach executes two statistical parameter optimization steps by using the benefits of error propagation formula. In future work, we intend to investigate the estimation of vertical vanishing point to accomplish camera calibration task.

6. REFERENCES

- Lu, F., Zhao, T. and Nevatia, R., 2000 Self-Calibration of a camera from video of a walking human. *in Proc. of ICPR*
- Criminisi, A., Reid, I. and Zisserman, A., 1999 Single view metrology. *in Proc. of ICCV*, pp. 434-442
- Hartley, R. and Zisserman, A., 2000 *Multiple View Geometry in Computer Vision*, University Press, Cambridge.
- Nguyen, V., Martinelli, A., Tomatis, N. and Siegart, R., 2005 A Comparison of Line Extraction Algorithms using 2D Laser Rangefinder for Indoor Mobile Robotics. *in Proc. of IROS*
- Ji, Q. and Xie, Y., 2003 Randomised hough transform with error propagation for line and circle detection. *Pattern Analysis and Applications*, vol. 6, pp. 55-64.
- Szlávik, Z., Havasi, L. and Szirányi, T., 2004 Estimation of common groundplane based on co-motion statistics. *in Proc. of Image Analysis and Recognition*, LNCS Springer, New York, pp. 347-353.
- Havasi, L. and Szirányi, T., 2006 Estimation of Vanishing Point in Camera-Mirror Scenes Using Video. *Optics Letters*, In Press. <http://digitus.itk.ppke.hu/~havasi/pev/ol.pdf>
- Kallenberg, O., 1997 *Foundations of Modern Probability*. New York: Springer-Verlag.
- Haralick, R.M., 1994 Propagating covariance in computer vision. *in Proc. of ICPR*, pp. 493-498.
- Kiryati, N. and Bruckstein, A. M., 2000 Heteroscedastic Hough Transform (HtHT): An Effective Method for Robust Line Fitting in the 'Errors in the Variables' Problem. *Computer Vision and Image Understanding*, vol. 78, pp. 69-83.
- Duda, R. O. and Hart, P. E., 1972 Use of the Hough transform to detect lines and curves in pictures. *Comm. ACM*, pp. 11-15.
- Stauffer C., Eric W. and Grimson L., 2000 Learning patterns of activity using real-time tracking. *IEEE Transactions on Pattern Analysis and Machine Intelligence*, vol. 22, pp. 747-757.
- Cucchiara R., Grana C., Piccardi M. and Prati A., 2003 Detecting Moving Objects, Ghosts and Shadows in Video Streams. *IEEE Transactions on Pattern Analysis and Machine Intelligence*, vol. 25, pp. 1337-1342.